ARTICLE

Theoretical Investigation of $CH_3CF_2O_2$+HOO Reaction

Xue-li Cheng[a*], Gui-xin Li[c], Zuo-mao Wang[b], Yan-yun Zhao[a,b], Yi-feng Sun[a]

a. Department of Chemistry, Taishan University, Tai'an 271021, China;
b. Department of Chemistry, Qufu Normal University, Qufu 273165, China;
c. Department of Philosophy, Taishan University, Tai'an 271021, China

(Dated: Received on September 29, 2006; Accepted on March 12, 2007)

The reactions of $CH_3CF_2O_2$ with HOO are important chemical cyclic processes of photochemical contamination. In this paper, the reaction pathways and reaction mechanism of $CH_3CF_2O_2$+HOO are investigated extensively with the Gaussian 98 package at the B3LYP/6-311++G** basis sets. The use of vibrational mode analysis and electron population analysis to reveal the reaction mechanism is firstly reported. The study shows that $CH_3CF_2CO_2$+HOO→IM1→TS1→$CH_3CF_2O_2H$+O_2 channel is the energetically most favorable, $CH_3CF_2CO_2H$ and O_2 are the principal products, and the formation of CH_3OH and CF_2O is also possible.

Key words: $CH_3CF_2CO_2$ radical, Vibrational mode analysis, Population analysis

I. INTRODUCTION

When freons are emitted to the atmosphere, they can affect the ozonosphere, and therefore some substitutes have been investigated. For its shorter life period in atmosphere and less greenhouse effect, CH_3CHF_2 may be used widely [1]. CH_3CHF_2 can react with hydroxyl free radical OH, forming $CH_3CF_2O_2$ [2,3]. The HOO radical is the main product of photooxidation processes of organic compounds in the atmosphere [4,5]. Moreover, the HOO radical is very active in photochemical reaction systems [6-9] and several reaction systems have been investigated [10-19]. The free radical reactions of $CH_3CF_2O_2$ with HOO are important chemical cyclic processes of photochemical contamination, but only a few experimental and theoretical studies have been reported [20,21]. Because $CH_3CF_2O_2$ and the intermediates and transition states involved in this reaction system have various configurations, it is necessary to carry out a theoretical investigation to elucidate the reaction mechanism.

Recently, elucidation of reaction mechanisms with a vibrational mechanism has attracted interests [22-24]. Along reaction coordinates, the vibrational frequencies of the same radical increase or decrease slightly because of different chemical environments provided by various compounds. Analyzing the changes in vibrational modes from reactant to transition states and from transition states to products can explain the direction of the reactions and degree of chemical reaction. But this approach cannot substitute completely for intrinsic reaction coordinate (IRC) calculations, especially for isomerization reactions, because the only imaginary frequency of a transition state is always related to the breaking or forming of bonds that are extended. Moreover, the number of imaginary frequencies can confirm whether there is a local minimum or a meta-stable state and transition state, so only the first or the lowest frequencies are essential to elucidate the reaction mechanism. Listing all vibrational frequencies provides more molecular information only. To summarize, the first or the lowest vibrational frequencies are sufficient to investigate a reaction mechanism using vibrational mode analysis.

II. COMPUTATIONAL METHOD

The Gaussian 98 program package [25] was employed to fully optimize all species involved in the reaction of $CH_3CF_2O_2$+HOO at the B3LYP/6-311++G** level. A B3LYP method, namely Becke's three-parameter nonlocal exchange functional [26] with the nonlocal correlation functional of Lee *et al.* [27], was used throughout the study. It is essential to employ a basis set that possesses sufficient diffuseness to obtain reliable properties for non-covalent interaction. Structures of all species were fully optimized prior to analytical second derivative calculations and vibrational analysis, and the number of imaginary frequencies (0 or 1) confirmed whether there was a local minimum or a transition state. Subsequently, connections of the transition states and products were confirmed by IRC calculations [28-30]. Zero-point vibrational energy (ZPVE, $1/2\sum h\omega_1$) scaling and thermal correction (TC) at 298.15 K were performed.

III. RESULTS AND DISCUSSION

The equilibrium structures of all species optimized at the B3LYP/6-311++G** level are shown in Fig.1. TS2, IM3, and TS3 have seven-atom twisting rings, and some species have no symmetric planes.

*Author to whom correspondence should be addressed. E-mail: x_cheng@tsu.edu.cn

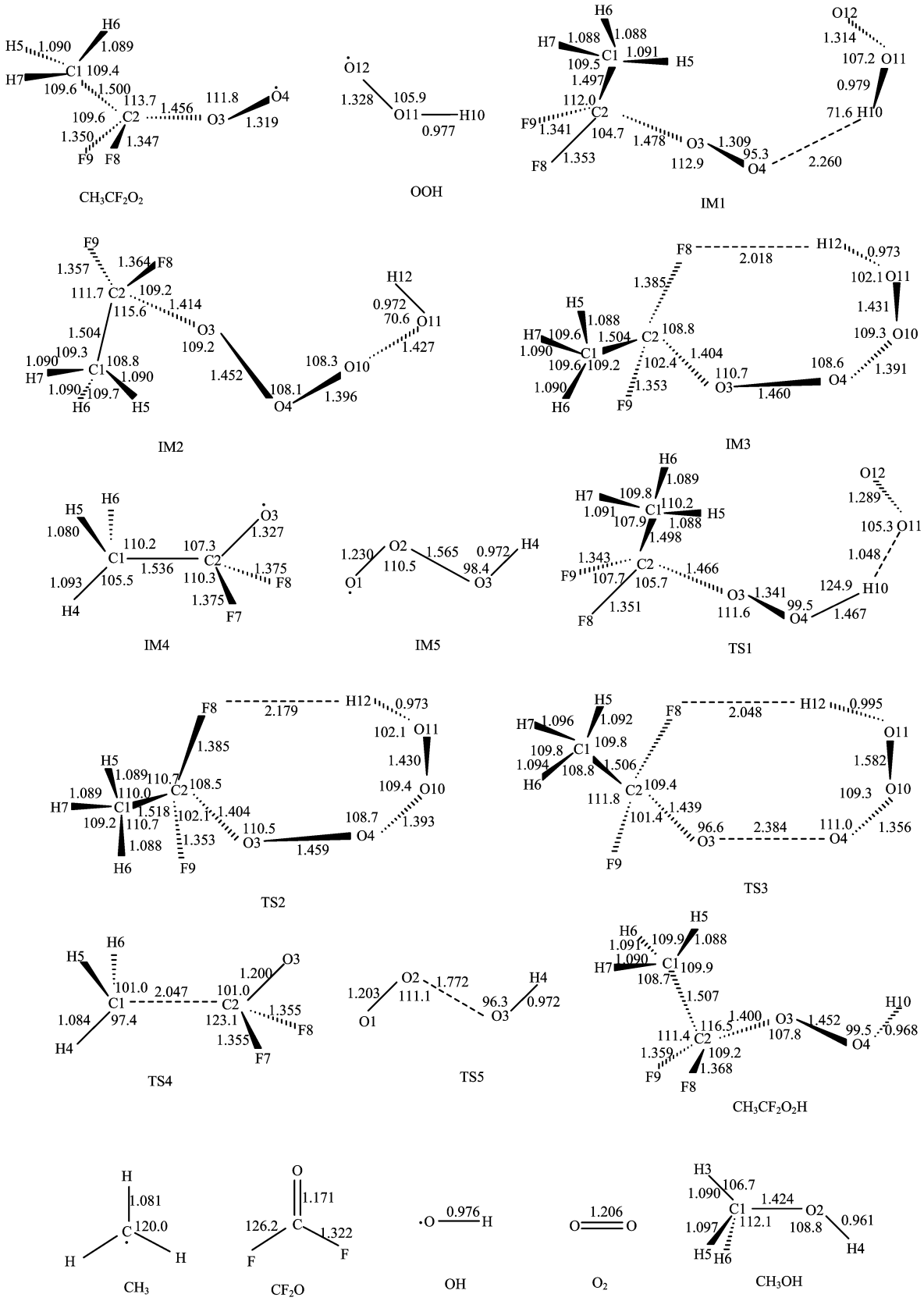

FIG. 1 B3LYP/6-311++G** optimized geometrical parameters for various species involved in the $CH_3CF_2O_2$+HOO reaction system. Bond lengths are in Å and bond angles in (°). Numbers besides atomic symbols are sequence numbers to distinguish them.

DOI:10.1088/1674-0068/20/03/243-248

TABLE I The dihedral angles of some species belonging to C_s group

Dihedral angle /(°)	$CH_3CF_2CO_2$	IM1	TS1	CH_3CF_2COOH	IM2	TS2	IM3	TS3
D(C1C2O3O4)	56.4	45.5	51.8	56.9	−55.6	47.0	46.1	53.4
D(H5C1C2O3)	179.4	−176.3	−60.3	−64.2	−176.9	−124.0	−64.1	−65.5
D(H6C1C2O3)	−60.8	−57.0	60.8	56.6	−57.2	−3.4	56.4	54.8
D(H7C1C2O3)	59.7	63.9	−179.6	176.1	63.3	116.4	175.9	174.2
D(F8C2O3O4)	−68.2	−78.1	−72.5	−68.8	70.2	−78.9	−79.4	−73.0
D(F9C2O3O4)	178.4	−177.2	174.9	178.4	−176.9	170.0	168.8	175.7
D(H10O4O3C2)		−127.9	−124.5	−132.7				
D(O11H10O4O3)		71.2	54.4					
D(O12O11H10O4)		−90.3	−68.2					
D(O10O4O3C2)					−96.4	103.6	103.7	81.5
D(O11O10O4O3)					−83.3	−95.5	−94.9	−89.3
D(H12O11O10O4)					91.8	89.4	89.6	89.3

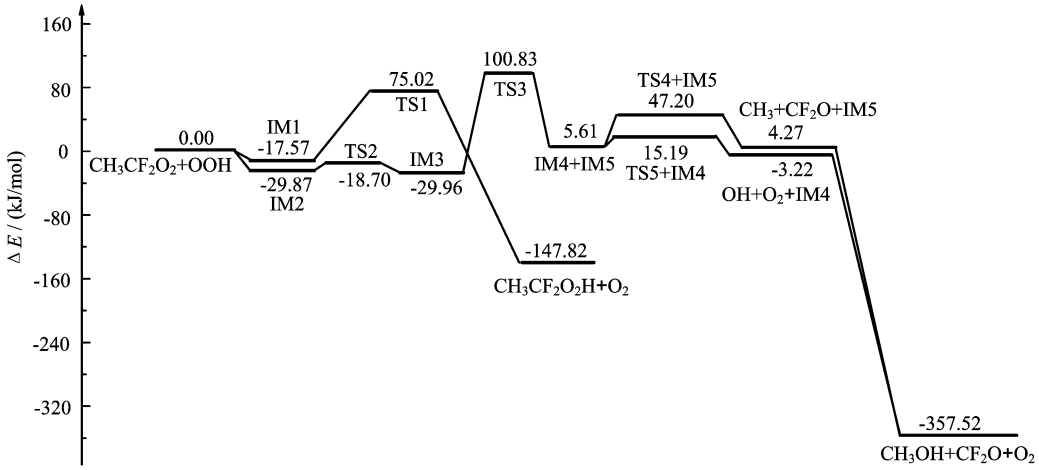

FIG. 2 Overall profile of potential energy surface for the $CH_3CF_2O_2$+HOO reaction system.

In order to show the geometries better, the dihedral angles of the species belonging to the C_s point group are shown in Table I. To clarify the reaction mechanism, the schematic potential energy profile is depicted in Fig.2.

A. Structural analysis

The H atom of the HOO radical can add to the O atom of $CH_3CF_2O_2$ and form IM1. The bond length of the newly formed O4−H10 is 2.260 Å. IM1 can decompose to $CH_3CF_2O_2H$ and O_2 via TS1, in which the breaking O11−H10 bond is extended to 1.048 Å, and the formed O4−H10 is shortened to 1.467 Å. In fact, this O4−H10 bond is a hydrogen bond. From the dihedral angles shown in Table I, it can be seen that all species in this channel are restricted to a similar structure.

The terminal O atom of HOO can also add to the O4 atom of $CH_3CF_2O_2$, forming IM2. Because the single electron is on O4 and O10, the new O4−O10 bond, with the bond length of 1.396Å, is shorter than a normal O−O single bond. IM2 can be isomerized to IM3 via TS2. The isomerization process results in distinct changes in dihedral angles. Because hydrogen bond forms between F8 and H12, TS2 and IM3 have seven-atom rings, with the bond lengths of 2.179 and 2.018 Å, respectively. IM3 will decompose to IM4 and IM5 via TS3. In TS3, the breaking O3−O4 bond is extended to 2.384 Å, and the F8−H2 hydrogen bond is also extended slightly.

IM4 will decompose to CH_3 and CF_2O via TS4. The C−C bond length of TS4 is extended to 2.047 Å. IM5 can also decompose to O_2 and O−H radical via TS5, and the breaking O−O bond length is extended to 1.772 Å. But these two decomposition processes cannot make the internal energy decrease effectively, as shown in Fig.2. However, when the CH_3 radical and the O−H radical form methanol via a non-barrier process, the relative energy is reduced to −357.69 kJ/mol.

DOI:10.1088/1674-0068/20/03/243-248

B. Vibrational analysis

All vibrational frequencies are assigned to six normal vibrational modes, viz. twist mode, rock out of plane (rock o.p.) mode, rock in plane (rock i.p.) mode, bend mode, symmetric stretch (symm. stretch) mode, and asymmetric stretch (asym. stretch) mode. For transition states, the only imaginary frequency of a transition state (TS) is always related to the breaking or forming bond that is extended. Moreover, the number of imaginary frequencies (0 or 1) can confirm whether a local minimum or a meta-stable state and TS. Because the non-planar constructions make frequencies hard to assign, so only the first or the lowest frequencies are essential to elucidate the reaction mechanism. The first frequencies of all species along with their vibrational mode assignment and IR intensity are listed in Table II.

TABLE II First frequency (cm^{-1}) and the vibrational mode assignment of all species (IR)

Species	Frequency	Intensity	Mode assignment
$CH_3CF_2CO_2$	108	1.0994	Molecule twist
OOH	1156	28.9093	O−O stretch
IM1	61	0.2376	Molecule rock o.p.
TS1	682i	51.4635	O11−H10 rock i.p.
$CH_3CF_2CO_2H$	114	2.4978	Molecule twist
O2	1633	0.0000	O−O stretch
IM2	54	4.3096	Molecule rock o.p.
TS2	225i	0.0389	O3−O−O rock i.p.
IM3	45	2.0959	Molecule rock o.p
TS3	268i	50.6626	O3−O4 stretch
IM4	174	0.0001	CH_3 twist
TS4	4537i	87.6718	C−C stretch
CH_3	5407	96.5335	CH_3 rock o.p.
CF_2O	576	5.8450	Molecule twist
IM5	165	129.0586	O−O−O−H rock o.p.
TS5	369i	34.4027	O2−O3 stretch
OH	3708	13.3556	O−H stretch
CH_3OH	297	134.7620	Molecule twist

From Table II, it can be seen that all reactants, intermediates and products have no imaginary frequencies, suggesting that they are local minima. The infrared intensity of homonuclear diatomic molecule O_2 is 0.0000. The only imaginary frequency of each transition state has relatively high IR intensity except for the isomerization process transition state TS2.

IM1 will decompose to $CH_3CF_2O_2H+O_2$ through the bond-breakage transition state TS1. The imaginary frequency of TS1 is assigned to the rock in plane mode of the breaking O11−H10 bond (682i cm^{-1}). The activation energy of this channel is 104.94 kJ/mol. IM2 can isomerize to IM3 via TS2. The imaginary frequency of TS2 belongs to the O3−O−O rock in plane mode because the structural adjustment of O3−O−O makes the seven-atom ring come into being. Via TS3, IM3 can decompose to IM4 and IM5 through the bond breakage of O3−O4; therefore the imaginary frequency of TS3 belongs to the O3−O4 stretch mode (268i cm^{-1}). For TS4, the imaginary frequency is assigned to the C−C stretch mode (453i cm^{-1}), which is related to the extended and broken C−C bond. The O2−O3 bond of TS5 will break and extend to 1.442 Å, so its imaginary frequency is the O2−O3 stretch mode at 368i cm^{-1}. Subsequently, the vibrational mode of a transition state verifies the connection between the transition state and product of each pathway.

C. Electron population analysis

Population analysis is a mathematical way of partitioning electron density into charges on the nuclei, bond orders, and other related information. These are probably the most widely used results that are not experimentally observable. Atomic charges cannot be observed experimentally because they do not correspond to any unique physical property [31]. For the $CH_3CF_2O_2$+ HOO reaction system, along with the reaction coordinate, the Mulliken charges of all species change accordingly. Electron population analysis can be used to analyze the reaction process to elucidate the reaction mechanism. The total atomic charges for all species are listed in Table III.

When the H10 atom of HOO is added to the O4 atom of $CH_3CF_2O_2$ to form IM1, the Mulliken charge on O4 becomes more negative; and along with the reaction coordinate the charge on O11 increases from −0.121 e to 0.077 e, becoming positively charged, indicating the hydrogen bonding species IM1 forms. The charges of other atoms are slightly changed accordingly. And when O11−H10 bond is breaking in TS1, O11 is again negatively charged (−0.009 e), suggesting that the induction effect of O11 atom becomes very weak. Then this bond breaks and the non-polar molecule O_2 forms.

In IM2, under the influence of electropositive atoms C2 and H12, the neighboring O3 and O11 are negatively charged, so O4 and O10 are slightly positively charged. The charges are readjusted because of the formation of a normal O4−O10 single bond. For the isomerization transition state TS2, all bond lengths only change slightly, so the charges also vary slightly. Along with the formation of IM3, the charges are readjusted. For TS3, the weak F8−H12 and O3−O4 bonds connect CH_3CF_2O to HOO. Since O4 and H12 are apart from O3 and F8, these two highly electronegative atoms F8 and O3 are more inclined to attract electrons. The sharp variety of charge in TS3 may suggest that this channel has relatively high potential energy. In fact, this potential is as high as 130.85 kJ/mol. IM4 and IM5 can decompose to smaller molecule segments via TS4 and TS5, respectively. In TS4, the negative charge

DOI:10.1088/1674-0068/20/03/243-248

TABLE III Mulliken charges on different atoms for all species involved in the $CH_3CF_2O_2$+HOO reaction system

Species	C1	C2	O3	O4	H5	H6	H7	F8	F9	H10	O11	O12
$CH_3CF_2CO_2$	−0.383	0.096	−0.025	−0.086	0.193	0.210	0.201	−0.108	−0.099			
OOH										0.267	−0.121	−0.146
IM1	−0.424	0.148	0.107	−0.308	0.183	0.224	0.210	−0.114	−0.082	0.257	0.077	−0.279
TS1	−0.428	0.135	0.061	−0.306	0.221	0.209	0.189	−0.106	−0.082	0.267	−0.009	−0.152
CH_3CF_2COOH	−0.441	0.151	−0.151	−0.157	0.207	0.196	0.189	−0.128	−0.122	0.256		
O_2											0.000	0.000
	C1	C2	O3	O4	H5	H6	H7	F8	F9	O10	O11	H12
IM2	−0.359	0.030	−0.212	0.089	0.188	0.209	0.198	−0.113	−0.105	0.061	−0.239	0.255
TS2	−0.354	0.104	−0.164	0.065	0.198	0.192	0.177	−0.176	−0.116	0.012	−0.191	0.254
IM3	−0.384	0.046	−0.159	0.070	0.200	0.214	0.188	−0.158	−0.189	0.023	−0.203	0.253
TS3	−0.512	0.981	−0.408	0.049	0.218	0.220	0.210	−0.455	−0.408	−0.056	−0.335	0.495
	C1	C2	O3	H4	H5	H6	F7	F8	O1	O2	O3	H4
IM4	−0.443	0.120	−0.042	0.207	0.205	0.205	−0.126	−0.126				
IM5									−0.102	0.139	−0.287	0.250
TS4	−0.437	0.123	−0.159	0.197	0.211	0.211	−0.073	−0.073				
TS5								−0.027	0.125	−0.335	0.237	
CH_3+CF_2O	−0.385	0.369	−0.216	0.128	0.128	0.128	−0.076	−0.076				
OH+O_2								0.000	0.000	−0.240	0.240	
CH_3OH	−0.279			0.149	0.120	0.120					−0.362	0.250

on O increases from −0.042 e to −0.159 e, indicating the fact that the oxygen atom that attracts electrons from C2 weakens the C−C bond. For TS3, the leaving O3 atom attracts fewer electrons from O2, and the negative charge on O1 decreases by 0.075 e. When the hydroxyl leaves O2 completely, charges on O1 and O2 are changed to 0.000, and a non-polar O_2 forms.

IV. CONCLUSION

CH_3CHF_2 may be used as a substitute for freons, but it can ultimately lead to environmental pollution. The reactions of its derivative $CH_3CF_2O_2$with HOO are important chemical cyclic processes of photochemical contamination. In this paper, the reaction pathways and reaction mechanism of $CH_3CF_2O_2$+HOO were investigated extensively with the Gaussian 98 package at the B3LYP/6-311++G** level. The relationship of the transition states and products were confirmed by IRC calculation. With the relative energies after TC and ZVPE corrections, the potential energy surface was drawn. The reaction mechanism was discussed, and vibrational mode analysis and electron population analysis were used to reveal the reaction mechanism for the first time. The PES shows that the $CH_3CF_2CO_2$+HOO→IM1→S1→$CH_3CF_2O_2H$+O_2 channel is the energetically most favorable, and the IM1 activated to TS1 process is the rate-determining step. Therefore, $CH_3CF_2O_2H$ and O_2 are the main products. The vibrational mode analysis and electron population analysis show that the decomposition of IM3 needs relatively high activation energy, and the formation of CH_3, CF_2O, OH and O_2 can not result in remarkable decrease of internal energy. Considering of the formation of CH_3OH, however, this pathway is possible. CH_3OH and CF_2O have been detected in Hashikawa's experiment [20].

V. ACKNOWLEDGMENT

This work was supported by the National Natural Science Foundation of China (No.10674099).

[1] J. T. Houghton, Y. Ding, and D. J. Griggs, *Climate Change 2001: The Scientific Basis*, Cambridge UK: Cambridge University Press, (2001).
[2] F. Taketani, T. Nakayama, K. Takahashi, Y. Matsumi, M. D. Hurley, T. J. Wallington, A. Toft, and M. P. S. Andersen, J. Phys. Chem. A Mol. Spectrosc. Kinet. Environ. Gen. Theory. **109**, 9061 (2005).
[3] F. Taketani, T. Nakayama, K. Takahashi, Y. Matsumi, M. D. Hurley, T. J. Wallington, A. Toft, and M. P. Sulbaek Andersen, J. Phys. Chem. A **109**, 9061 (2005).
[4] G. P. Brasseur, J. J. Orlando, and G. S. Tyndall, *Atmospheric Chemistry and Global Change*, New York: Oxford University Press, (1999).
[5] G. S. Tyndall, R. A. Cox, C. Granier, R. Lesclaux, G. K. Moortgat, M. J. Pilling, A. R. Ravishankara, and T. J. Wallington, J. Geophys. Res. **106**, 157 (2001).
[6] C. J. Chen and J. W. Bozzelli, J. Phys. Chem. A **103**, 9731 (1999).
[7] T. P. W. Jungkamp, J. N. Smith, and J. H. Seinfeld, J. Phys. Chem. **101**, 4392 (1997).

DOI:10.1088/1674-0068/20/03/243-248

[8] T. H. Lay and J. W. Bozzelli, J. Phys. Chem. **101**, 9505 (1997).
[9] T. M. Lenhardt, C. E. Mcdade, and K. D. Bayes, J. Chem. Phys. **94**, 8 (1990).
[10] R. Sommariva, W. J. Bloss, N. Brough, N. Carslaw, M. Flynn, A. L. Haggerstone, D. E. Heard, J. R. Hopkins, J. D. Lee, A. C. Lewis, G. McFiggans, P. S. Monks, S. A. Penkett, M. J. Pilling, J. M. C. Plane, K. A. Read, A. Saiz-Lopez, A. R. Rickard, and P. I. Williams, Atmos. Chem. Phys. **6**, 1135 (2006).
[11] H. T. Bai, X. R. Huang, Z. G. Wei, J. L. Li, and J. Z. Sun, Acta Chim. Sin. **63**, 196 (2005).
[12] C. X. Cui, W. C. L, Z. S. Li, and J. Z. Sun, Chem. J. Chin. Univ. **24**, 872 (2003).
[13] H. T. Bai, X. R. Huang, J. K. Yu, J. L. Li, and C. C. Sun, Chem. J. Chin. Univ. **26**, 697 (2005).
[14] M. Shao, X. R. Ren, H. X. Wang, L. M. Zeng, Y. H. Zhang, and X. Y. Tang, Chin. Sci. Bull. **49**, 2253 (2004).
[15] H. Hua and B. S. Wang, Chem. Phys. Lett. **410**, 235 (2005).
[16] H. Hua, J. C. Li, X. L. Song, and B. S. Wang, J. Phys. Chem. A **109**, 11206 (2005).
[17] H. Hua, L. Z. Deng, J. C. Li, and B. S. Wang, J. Phys. Chem. A **109**, 9299 (2005).
[18] H. Hua and B. S. Wang, J. Phys. Chem. A **109**, 451 (2005).
[19] G. X. Li and J. L. Li, J. Mol. Catal. (China) **5**, 233 (1991).
[20] Y. Hashikawa, M. Kawasaki, M. P. S. Andersen, M. D. Hurley, and T. J. Wallington, Chem. Phys. Lett. **391**, 165 (2004).
[21] L. C. Li, Y. Q. Zhu, D. Zha, and A. M. Tian, Acta Phys. Chim. Sin. **21**, 490 (2005).
[22] X. L. Cheng, L. Niu, Y. Y. Zhao, and Z. Zhou, Spectrochim. Acta A **60**, 907 (2004).
[23] X. L. Cheng, J. Mol. Stru. (Theochem) **731**, 89 (2005).
[24] X. L. Cheng, Z. Y. Zhou, Y. Y. Zhao, Y. F. Sun, and Y. Zhu, J. Mol. Stru. (Theochem) **725**, 103 (2005).
[25] M. J. Frisch, G. W. Trucks, H. B. Schlegel, G. E. Scuseria, M. A. Robb, J. R. Cheeseman, V. G. Zakrzewski, J. A. Montgomery Jr., R. E. Stratmann, J. C. Burant, S. Dapprich, J. M. Millam, A. D. Daniels, K. N. Kudin, M. C. Strain, O. Farkas, J. Tomasi, V. Barone, M. Cossi, R. Cammi, B. Mennucci, C. Pomelli, C. Adamo, S. Clifford, J. Ochterski, G. A. Petersson, P. Y. Ayala, Q. Cui, K. Morokuma, D. K. Malick, A. D. Rabuck, K. Raghavachari, J. B. Foresman, J. Cioslowski, J. V. Ortiz, B. B. Stefanov, G. Liu, A. Liashenko, P. Piskorz, I. Komaromi, R. Gomperts, R. L. Martin, D. J. Fox, T. Keith, M. A. Al-Laham, C. Y. Peng, A. Nanayakkara, C. Gonzalez, M. Challacombe, P. M. W. Gill, B. Johnson, W. Chen, M. W. Wong, J. L. Andres, C. Gonzalez, M. Head-Gordon, E. S. Replogle, and J. A. Pople, *Gaussian 98*, Revision A.7. Pittsburgh PA: Gaussian Inc. (1998)
[26] A. D. Becke, J. Chem. Phys. **98**, 5648 (1993).
[27] C. Lee, W. Yang, and R. G. Parr, Phys. Rev. B **37**, 785 (1988).
[28] K. Fukui, S. Kato, and H. Fujimoto, J. Am. Chem. Soc. **97**, 1 (1975).
[29] K. Ishida, K. Morokuma and A. Komornicki, J. Chem. Phys. **66**, 2153 (1977).
[30] Z. Gonzalez and H. B. Schlegel, J. Phys. Chem. **90**, 2154 (1989).
[31] D. C. Young, *Computational Chemistry: A Practical Guide for Applying Techniques to Real-World Problems*, New York: John Wiley & Sons, 99 (2001).

DOI:10.1088/1674-0068/20/03/243-248